JOURNAL OF GEOPHYSICAL RESEARCH, VOL. 115, D18118, doi:10.1029/2009JD013010, 2010

Seasonal persistence of ozone and zonal wind anomalies in the equatorial stratosphere

S. Tegtmeier,[1,2] V. E. Fioletov,[1] and T. G. Shepherd[3]

Received 13 August 2009; revised 17 March 2010; accepted 30 March 2010; published 25 September 2010.

[1] Analysis of the variability of equatorial ozone profiles in the Satellite Aerosol and Gas Experiment-corrected Solar Backscatter Ultraviolet data set demonstrates a strong seasonal persistence of interannual ozone anomalies, revealing a seasonal dependence to equatorial ozone variability. In the lower stratosphere (40–25 hPa) and in the upper stratosphere (6–4 hPa), ozone anomalies persist from approximately November until June of the following year, while ozone anomalies in the layer between 16 and 10 hPa persist from June to December. Analysis of zonal wind fields in the lower stratosphere and temperature fields in the upper stratosphere reveals a similar seasonal persistence of the zonal wind and temperature anomalies associated with the quasi-biennial oscillation (QBO). Thus, the persistence of interannual ozone anomalies in the lower and upper equatorial stratosphere, which are mainly associated with the well-known QBO ozone signal through the QBO-induced meridional circulation, is related to a newly identified seasonal persistence of the QBO itself. The upper stratospheric QBO ozone signal is argued to arise from a combination of QBO-induced temperature and NO_x perturbations, with the former dominating at 5 hPa and the latter at 10 hPa. Ozone anomalies in the transition zone between dynamical and photochemical control of ozone (16–10 hPa) are less influenced by the QBO signal and show a quite different seasonal persistence compared to the regions above and below.

Citation: Tegtmeier, S., V. E. Fioletov, and T. G. Shepherd (2010), Seasonal persistence of ozone and zonal wind anomalies in the equatorial stratosphere, *J. Geophys. Res.*, *115*, D18118, doi:10.1029/2009JD013010.

1. Introduction

[2] The quasi-biennial oscillation (QBO) in tropical zonal wind is the dominant influence on the interannual variability of equatorial total ozone [e.g., *Funk and Garnham*, 1962; *Ramanathan*, 1963]. The QBO signal in total ozone varies between ±4% of the background total column amount and is approximately in phase with the zonal wind at 20–30 hPa (24–27 km) [e.g., *Hasebe*, 1983; *Bowman*, 1989; *Randel and Cobb*, 1994; *Tung and Yang*, 1994]. Long-term records of ozone profile measurements make it possible to investigate the vertical structure of ozone anomalies and demonstrate that the tropical ozone QBO has a double peaked structure in the vertical with maxima in the lower (20–27 km) and middle/upper (30–37 km) stratosphere [*Zawodny and McCormick*, 1991; *Hasebe*, 1994]. The boundary between dynamical and photochemical control of ozone around 28–30 km is apparent from this structure. Below 28 km, O_x has a long lifetime [*Brasseur and Solomon,* 2005], and ozone is mainly under dynamical control. It follows that the QBO signal in lower stratospheric ozone results from the transport of ozone by the QBO-induced meridional circulation. Above 30 km, on the other hand, O_x has a short lifetime and ozone is under photochemical control. The QBO signal in middle/upper stratospheric ozone is thus understood to arise not from transport of ozone itself but from QBO-induced temperature variations [*Ling and London*, 1986; *Zawodny and McCormick*, 1991] together with QBO-induced variability in the transport of NO_y that affects ozone chemically through NO_x [*Chipperfield et al.*, 1994; *Tian et al.*, 2006].

[3] It is well established that the variability of extratropical ozone anomalies is related to the variability of the dynamical forcing of the Brewer-Dobson circulation [*Fusco and Salby*, 1999; *Randel et al.*, 2002; *Weber et al.*, 2003], which is affected by the QBO [*Holton and Tan*, 1980]. An important characteristic of the QBO signal in extratropical total ozone is its seasonal synchronization [*Randel and Wu*, 1996], with maxima in the winter-spring hemisphere. *Fioletov and Shepherd* [2003] showed that interannual midlatitude total ozone anomalies established in winter/spring persist through the summer until the next autumn. *Tegtmeier et al.* [2008] found that the Northern Hemisphere (NH) subtropical partial ozone column above 16 hPa shows especially strong seasonal persistence and argued on the basis of analysis of other trace species that the ozone anomaly persistence arises from the persistence of transport-induced wintertime anomalies in NO_y, which perturb ozone through NO_x chemistry. The study implied that through this

[1]Environment Canada, Toronto, Ontario, Canada.
[2]Now at Marine Meteorology, IFM-GEOMAR, Kiel, Germany.
[3]Department of Physics, University of Toronto, Toronto, Ontario, Canada.

0148-0227/10/2009JD013010

"seasonal memory," the QBO has an asynchronous effect on subtropical ozone in the upper stratosphere during summer and early autumn. The seasonal persistence of lower stratospheric ozone is less strong and is related to the link between winter-spring ozone buildup due to transport of ozone itself and subsequent slow chemical decay of the anomalies in the dynamically quiescent summer stratosphere [*Fioletov and Shepherd*, 2003; *Tegtmeier et al.*, 2008].

[4] The seasonal persistence of ozone anomalies is of interest since it can be used to reconstruct missing data. For example, the especially strong seasonal persistence of extratropical upper stratospheric ozone anomalies means that most of the ozone variability in late spring, summer, and autumn can be described by the ozone variability during winter and early spring and results in excellent prediction capabilities, as demonstrated by *Tegtmeier et al.* [2008]. This capability can be useful for improving satellite ozone data sets by filling data gaps in the summer half of the year or ensuring the physical consistency of the data set.

[5] In contrast to the QBO signal in extratropical ozone, the QBO signal in equatorial total ozone is not synchronized with the annual cycle. There is no apparent preferred season in which the anomalies change sign or reach their maximum amplitudes [*Baldwin et al.*, 2001]. However, the QBO of the equatorial zonal winds, which as discussed above causes the equatorial ozone anomalies through the QBO-induced meridional circulation, is somewhat synchronized with the seasonal cycle in that the timing of QBO phase transitions displays a weak seasonal dependence [*Dunkerton and Delisi*, 1985; *Dunkerton*, 1990; *Pascoe et al.*, 2005]. It is not known with certainty what mechanism causes the seasonality of the QBO phase transitions; however, it is of interest to ask if this characteristic can lead to a seasonality of the ozone anomaly persistence. Moreover, it seems possible that the zonal wind anomalies may themselves be characterized by a seasonal persistence.

[6] In this study we therefore analyze the persistence of equatorial upper and lower stratospheric ozone anomalies, as well as the persistence of zonal wind anomalies, using the same approach as *Fioletov and Shepherd* [2003]. Data sets and methods are described in section 2. In section 3 the persistence of ozone and zonal wind anomalies based on correlation functions is presented. The section is structured into the analysis of ozone and zonal wind in the lower stratosphere, ozone in the middle/upper stratosphere, and ozone in the transition region between the lower and middle/upper stratosphere. A summary is provided in section 4.

2. Data and Methods

2.1. SAGE Data Set

[7] The Satellite Aerosol and Gas Experiment (SAGE) measurements [*McCormick et al.*, 1989; *Zawodny and McCormick*, 1991] were obtained through the solar occultation technique. The SAGE II sensor aboard the Earth Radiation Budget Satellite measured up to 14 sunrise and sunset profiles per day, which results in approximately 800 profiles per month. Spatial sampling is limited due to the satellite orbit, and data records for the tropics and/or midlatitudes have substantial gaps for individual months of the year. Validation studies have demonstrated the good quality of the SAGE I and SAGE II data records with an estimated precision of around 10% for SAGE I and 4–8% for SAGE II [*Cunnold et al.*, 1989; *Fioletov et al.*, 2006]. The SAGE data set has been used to compile the SAGE-corrected Solar Backscatter Ultraviolet (SBUV) ozone data set, which is the main focus of our paper. Additionally, the ozone and nitrogen dioxide (NO_2) data from the SAGE II sensor for the period from January 1985 to December 2003 processed with the version 6.2 retrieval algorithm [*Rind et al.*, 2005] are analyzed here. NO_2 data are based on sunset observations only to avoid systematic differences between sunrise and sunset concentrations.

2.2. SAGE-Corrected SBUV Ozone Data Set

[8] The seasonal persistence of ozone anomalies is estimated from the SAGE-corrected SBUV ozone data set [*McLinden et al.*, 2009]. The data set is based on a combination of Solar Backscatter Ultraviolet (SBUV) instrument and SAGE measurements, where the daily nearly global coverage of the first, and the precision and stability of the second, have been combined.

[9] The SBUV and SBUV2 instruments were launched on a sequence of NOAA satellites (7, 9, 11, 14, 16, 17, and 18). Together, they have been providing measurements with daily near-global coverage from 1978 to present. Differences between the individual SBUV(/2) instruments have been shown to lead to biases between the corresponding time series during the overlapping periods [*Frith et al.*, 2004]. Removing those biases has proven to be a challenge since the overlapping periods are sometimes short and the biases vary with time. Also, the SBUV algorithm can cause a damping of ozone fluctuations with fine vertical structure [*Bhartia et al.*, 2004]. As a result, the expected downward propagation of the equatorial QBO ozone signal is not properly captured in the SBUV(/2) data sets [*McLinden et al.*, 2009]. It is possible to correct the biases between the individual SBUV data sets with the help of a high-quality ozone data set from a stable source spanning roughly the same time frame as the SBUV(/2) data sets. Such data are provided by the SAGE I and SAGE II data sets.

[10] Differences between coincident measurements by SAGE and SBUV(/2) have been used for a bias correction of the individual SBUV(/2) instruments [*McLinden et al.*, 2009]. The SAGE-corrected SBUV data are based on SBUV(/2) data version 8.0 [*Bhartia et al.*, 2004], SAGE I version 7.0 and SAGE II version 6.2 [*Wang et al.*, 2006]. As a result of the corrections, the new data set shows a realistic downward propagation of the equatorial QBO ozone signal, in contrast to the original SBUV(/2) time series. The SAGE-corrected SBUV data set is provided as monthly zonal mean ozone spanning 1978–2005, limited by the end of SAGE II operations. The ozone profile data are given as partial ozone columns in Dobson Units (DU) for 12 layers, each approximately 3.2 km thick. The monthly zonal mean ozone profiles are provided in 5° wide latitude bands covering 80°S–80°N. Data are excluded for 10°S–30°N for the time period March 1982 to February 1983 following the eruption of El Chichon and for 20°S–30°N for the time period June 1991 to May 1992 following the eruption of Mt. Pinatubo.

2.3. HALOE Data Set

[11] The Halogen Occultation Experiment (HALOE) measurement technique is based on solar occultation with

daily observations of up to 15 sunrise and 15 sunset profiles. The HALOE instrument [*Russell et al.*, 1993] aboard the Upper Atmosphere Research Satellite observed mixing ratios of a number of trace gases including NO and NO_2 from 1991 to 2005. The HALOE data set used in this study is a set of monthly mean values covering the time period from October 1991 to August 2002 prepared by *Grooß and Russell* [2005]. The most recent data have not been included in this data set since the observations were much less frequent after 2002. The data are averaged over 5° wide equivalent latitude bins. The mixing ratio profiles of the trace species are given for 22 pressure levels between 316 and 0.1 hPa. We focus in this study on equatorial NO_x at the pressure level 5 hPa. The NO_x profile is calculated as the sum of the measured NO and NO_2 and is based on sunset events only.

2.4. Wind and Temperature Data

[12] The Free University of Berlin (FUB) QBO zonal wind data set [*Naujokat*, 1986] is based on daily radiosonde measurements in the tropics. Equatorial monthly zonal mean wind profiles were derived based on the daily measurements at three equatorial stations. The profiles are given for seven pressure levels between 70 and 10 hPa and cover the time period from 1953 to present.

[13] The temperature data set used here is obtained from the European Centre for Medium-Range Weather Forecasts (ECMWF) Reanalysis (ERA-40) [*Uppala et al.*, 2005]. We focus on monthly mean zonal mean temperature time series from 1978 to 2002 at 5 and 10 hPa.

2.5. Methods

[14] The main goal of this paper is to quantify the seasonal persistence of equatorial ozone profile anomalies in various stratospheric layers. The persistence of ozone anomalies can be measured by the correlation coefficient between the ozone anomalies in one month and the anomalies in another month. Therefore, we calculate the correlations between time series of partial ozone columns for individual months following the approach introduced by *Fioletov and Shepherd* [2003] for the total ozone column. The seasonal cycle and the long-term trend are removed from the original data prior to the calculation of the correlation coefficients. The long-term trend is estimated separately for each month of the year by fitting the ozone time series to the equivalent effective stratospheric chlorine (EESC) loading in the equatorial stratosphere. The EESC term is a measure of the stratospheric halogen burden and is used to isolate long-term ozone changes associated with the amount of ozone depleting chlorine and bromine in the stratosphere.

[15] Let x and y be the partial ozone column in two particular months and layers. The correlation coefficient between x and y equals

$$r_{xy} = \frac{\sum_{i=1}^{n-k} x_i y_{i+k}}{\sqrt{\sum_{i=1}^{n-k} x_i^2}\sqrt{\sum_{i=1}^{n-k} y_{i+k}^2}},$$

where x_i and y_i are the ozone anomalies in year i and n is the number of years in the record. Correlation coefficients between the 27 year time series greater than 0.4 are statistically significant at the 95% confidence level based on the Student's t test.

[16] A statistical regression analysis of the SAGE-corrected SBUV ozone data set is used to separate the ozone variability associated with the QBO from the ozone variability not explained by the QBO. For this application, which is used only to supplement the main analysis, the ozone time series for each layer were fit with a regression model including EESC, solar cycle, QBO, and El Nino-Southern Oscillation (ENSO) as explanatory variables [*World Meteorological Organization*, 2007, and references therein]. The QBO time series are based on observed equatorial winds at 30 and 50 hPa, and the solar cycle term is the standard $F_{10.7}$ radio flux. The regression model includes a constant and an annual harmonic term for the regression coefficients of the EESC and QBO function. The regression coefficients for the QBO functions estimated by the linear regression analysis are used to calculate the ozone anomalies purely associated with the QBO signal as a linear combination of the two QBO time series. The residual time series is considered to represent all the ozone variability not associated with the QBO signal.

3. Ozone Variations in the Equatorial Region

[17] Figure 1a shows equatorial ozone anomalies derived from the SAGE-corrected SBUV ozone data set. Only the portion from 1993 to 2002 of the 27 year long data set is displayed. The seasonal cycle has been removed from the monthly zonal mean ozone data averaged over 5°S–5°N, and the anomalies are displayed as percentages of the multiyear mean. The variability of equatorial ozone is dominated by the QBO signal with its characteristic alternating positive and negative anomalies that can be traced downward in time [*Zawodny and McCormick*, 1991; *Hasebe*, 1994; *Randel and Wu*, 1996]. The equatorial ozone QBO signal is seen to have a double peaked structure in the vertical with maxima in the lower (70–16 hPa, corresponding to 20–27 km) and middle/upper (10–4 hPa, corresponding to 30–37 km) stratosphere, as noted earlier. To simplify matters, we will refer to the partial ozone column below 16 hPa as lower stratospheric ozone and to the partial ozone column above 10 hPa as upper stratospheric ozone. In the dynamically controlled lower stratosphere, a westerly shear in QBO phase leads to a positive ozone anomaly, whereas in the photochemically controlled upper stratosphere, a westerly shear in QBO phase leads to a negative ozone anomaly. In order to analyze the persistence of ozone anomalies, we focus here on these two quite distinctive regions as well as the transition zone between them: the dynamically controlled region below 16 hPa is represented by SBUV(/2) layer 3 (corresponding to the partial ozone column between 40 and 25 hPa) and layer 2 (64–40 hPa), the photochemically controlled region above 10 hPa is represented by layer 7 (6–4 hPa), and the transition zone between the dynamically and photochemically controlled regions is represented by layer 5 (16–10 hPa).

[18] Standard deviations of the equatorial monthly zonal mean ozone anomalies for layers 3, 5, and 7 are shown in percent in Figure 1b. Ozone anomalies in layer 3 show the largest variability compared to the other two layers with values between 5% and 9%. The seasonal cycle of vari-

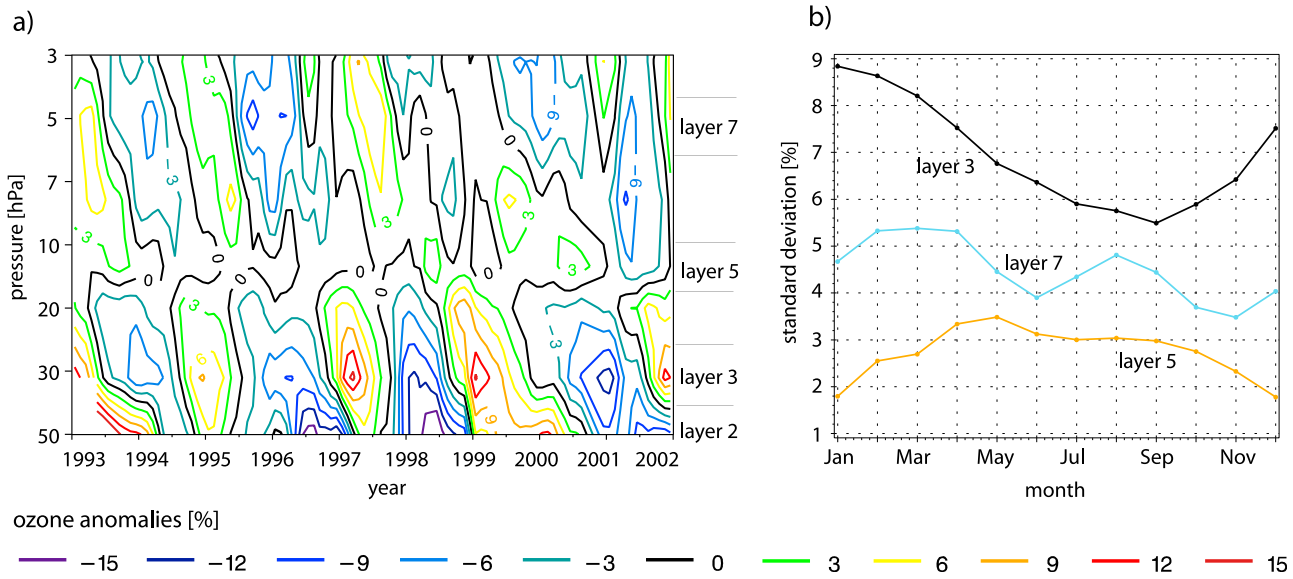

Figure 1. (a) Pressure-time section of interannual ozone anomalies from 1993 to 2002 averaged over 5°S–5°N from the SAGE-corrected SBUV data set. (b) Seasonal cycle of the standard deviation of ozone anomalies averaged over 5°S–5°N for the SAGE-corrected SBUV data set for the partial ozone column between 40 and 25 hPa (layer 3, black), 16 and 10 hPa (layer 5, orange), and 6 and 4 hPa (layer 7, blue).

ability for layer 3 has a maximum in January and a minimum in September. Ozone anomalies in layer 5 have the smallest relative standard deviations compared to the other two layers and a completely different seasonal cycle that peaks in late spring/summer. This is probably due to the fact that the QBO signals influencing ozone anomalies in layer 3 and in layer 7 cancel each other out in layer 5.

3.1. Ozone Persistence in the Equatorial Lower Stratosphere

[19] First, we analyze the persistence of equatorial ozone anomalies in the lower stratosphere, where ozone is under dynamical control. Figure 2a shows correlation coefficients between the ozone time series of layer 3 (40–25 hPa) for different months of the year. Each field of the frame represents the correlation coefficient between the monthly mean ozone anomaly time series for the month indicated on the *x* axis and that indicated on the *y* axis. Note that through the choice of the months on the *x* and *y* axis, the frame shows a symmetric structure with a diagonal representing correlation coefficients between the ozone time series of the same months, which equal 1. Clearly, there is a strong seasonal structure to the anomaly persistence: the monthly mean ozone anomalies for November/December are highly correlated with all the ozone anomalies in the following months until July. This pattern of correlation coefficients

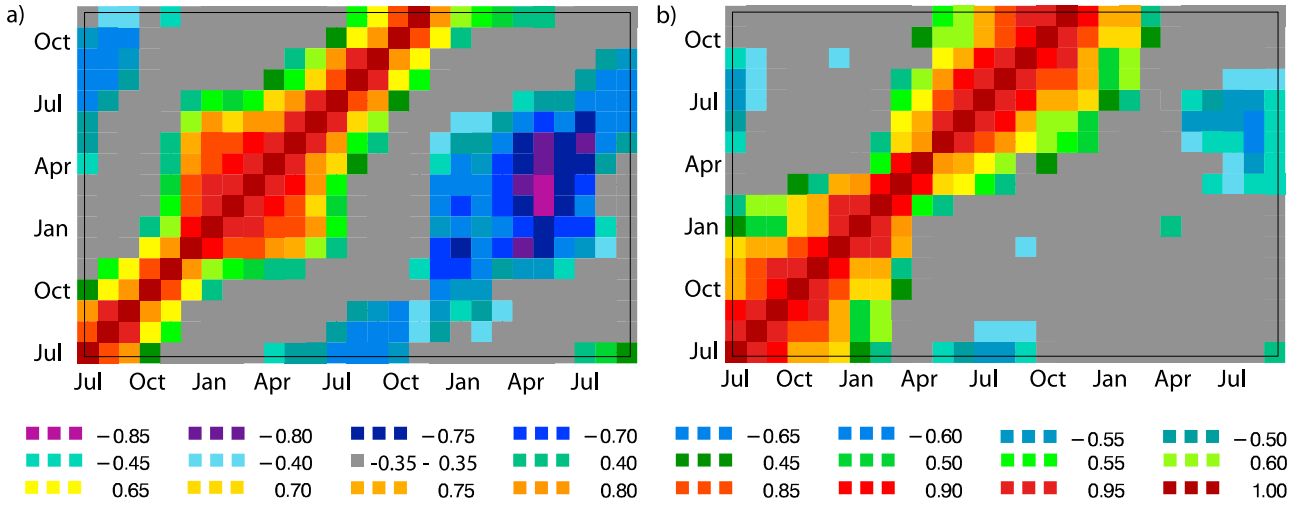

Figure 2. Correlation coefficients for ozone averaged over 5°S–5°N for the SAGE-corrected SBUV data set between monthly mean time series in (a) layer 3 and (b) layer 2. Each field represents the correlation between the ozone time series for two particular months, as labeled.

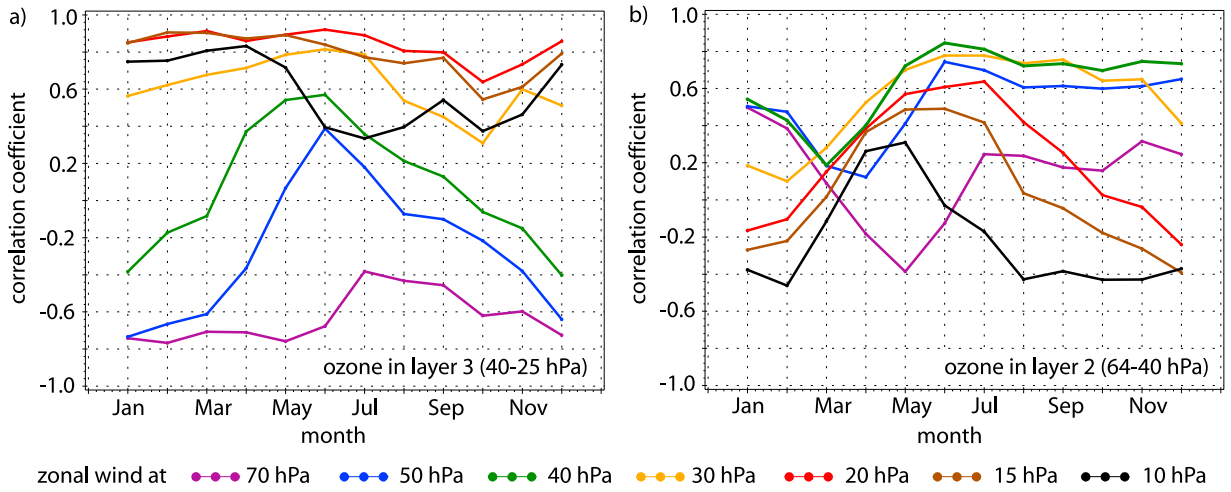

Figure 3. Correlation coefficients between FUB equatorial zonal wind and ozone averaged over 5°S–5°N for SAGE-corrected SBUV for (a) ozone in layer 3 (40–25 hPa) and (b) ozone in layer 2 (64–40 hPa). The pressure level of the zonal-wind anomaly is indicated by the color scale.

indicates that ozone anomalies in layer 3 get established in the NH autumn and then persist until the NH summer of the following year. A general characteristic of equatorial ozone is the alternating sign of the QBO ozone signal, which leads to a strong anticorrelation between anomalies separated by approximately 1 year. This is confirmed by the high negative correlation coefficients with values between −0.5 and −0.85 in Figure 2a. The pattern of strong negative correlation coefficients has a seasonal structure with especially strong negative correlations persisting between December and July, in a manner very similar to the pattern of high positive correlation coefficients. Both patterns of seasonal structure are quite surprising since the QBO signal in equatorial ozone is not assumed to be synchronized with the annual cycle [*Baldwin et al.*, 2001, and references therein]. Assuming that the ozone QBO dominates the variability of equatorial ozone, the correlation coefficients should decrease steadily to zero in a quarter of the 28 month period, i.e., in approximately 7 months. Thus, one would expect high correlation coefficients for only a few months, as is observed for the time frame from July to October. For the rest of the calendar year, however, our current understanding of the ozone QBO cannot explain either the 7–8 month long persistence of the ozone anomalies or the synchronization of this persistence with the seasonal cycle.

[20] Figure 2b shows the correlation coefficients between the monthly mean ozone anomaly time series of layer 2 (64–40 hPa). For this level, there is a time frame, roughly from July to December, characterized by an enhanced persistence relative to the persistence expected on the basis of the QBO period. A sharp drop of the correlation coefficients after February/March reveals a time with reduced persistence in late winter. The coefficients lagged by 1 year show only weak anticorrelations with values between −0.6 and −0.3. This might be related to the fact that the period of the ozone QBO is less regular at this lower level. The ERA-40 equatorial temperature anomalies (not shown here), which reflect the QBO-induced circulation anomalies, show a strong anticorrelation in the 1 year-lag coefficients at 20 hPa but no anticorrelation at 50 hPa, consistent with the behavior of the ozone correlations, which supports this hypothesis. Although the correlation coefficients in layer 2 show a completely different pattern than the coefficients in layer 3, both layers are characterized by a seasonal persistence of ozone anomalies during certain times of the calendar year.

[21] It is understood that equatorial ozone anomalies in the lower stratosphere are mainly forced by the vertical component of the QBO-induced meridional circulation that is required to generate the equatorial temperature signals associated with the vertical shear of the zonal wind [*Baldwin et al.*, 2001, and references therein]. To directly link equatorial ozone anomalies and zonal wind anomalies, we calculate correlation coefficients between the two fields for particular stratospheric levels. Figure 3a shows the seasonal cycle of correlations between ozone in layer 3 (40–25 hPa) and the zonal wind at seven individual levels between 70 and 10 hPa. The correlations maximize for the zonal wind at 20 hPa, which is slightly above the layer of the ozone anomalies. The high correlation coefficients with values between 0.7 and 0.9 indicate that the main characteristics of the time series of the zonal wind at 20 hPa will be reflected in the time series of equatorial ozone anomalies in layer 3. Figure 3b shows the correlations between ozone in layer 2 (64–40 hPa) and the zonal winds. Here the correlations maximize for the zonal wind at 40 hPa, which is the upper boundary of the ozone layer. The correlations are statistically significant for all months except March and show high values around 0.8 from May to December.

[22] Analysis of zonal winds in the equatorial stratosphere has shown that the period of the QBO varies on decadal time scales and that the timing of the QBO phase transition displays a weak seasonal dependence [*Dunkerton and Delisi*, 1985; *Dunkerton*, 1990], although the latter also varies on decadal time scales [*Anstey and Shepherd*, 2008]. Possible mechanisms to explain the seasonality of the timing of the phase transition include the semiannual oscillation, which might influence the initiation of QBO phases [*Dunkerton and Delisi*, 1985; *Campbell and Shepherd*, 2005], and the rate of phase progression of the QBO. The latter describes the rate at which successive easterly and westerly wind regimes

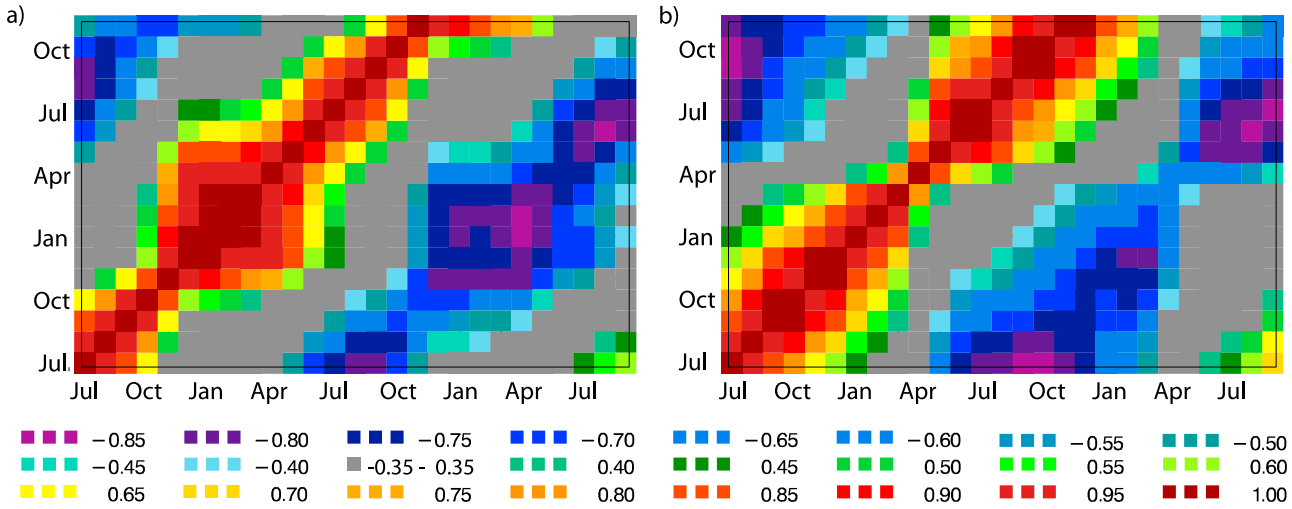

Figure 4. Correlation coefficients for FUB equatorial zonal wind between monthly mean time series at (a) 20 hPa and (b) 40 hPa. Each field represents the correlation between the zonal wind time series for two particular months, as labeled.

descend and has been shown to be strongly modulated by the seasonal cycle [*Dunkerton*, 1990; *Wallace et al.*, 1993]. The latter study demonstrated that the mean rate of phase progression is three times as large for the time frame from April to June compared to November to February. It is not known with certainty what mechanism causes the seasonality of the QBO phase transition; however, it seems possible that this mechanism could at the same time lead to a seasonal persistence in the equatorial zonal winds.

[23] In order to test if the zonal winds are characterized by a seasonal persistence, we calculate the correlation coefficients between the monthly zonal wind time series for particular stratospheric levels. Figure 4a shows the correlation coefficients between the zonal wind time series at 20 hPa for different months of the year. The zonal wind anomalies for all the months from November onward are highly correlated with the wind anomalies in the following months up to June/July. Thus, the pattern of high correlation coefficients reveals a 8–9 month long seasonal persistence of the equatorial zonal wind anomalies at 20 hPa. Figure 4b shows the correlation coefficients between the monthly mean zonal wind time series at 40 hPa. The most prominent feature here is a sharp drop of the correlation coefficients after March illustrating a reduced zonal wind anomaly persistence in late winter. From August to December, we find an enhanced persistence relative to the persistence expected on the basis of the QBO period. Thus, both stratospheric levels are characterized by a seasonal persistence of zonal wind anomalies and therefore a seasonal persistence of the QBO signal during certain times of the calendar year. However, the correlation coefficients at 40 hPa show a different time frame of persistence than the coefficients at 20 hPa, suggesting that the mechanism for the seasonal persistence is not related in any simple way to the seasonal cycle of tropical upwelling.

[24] We hypothesize that the seasonal persistence of zonal wind anomalies causes the seasonal persistence of the ozone anomalies. Analysis of the zonal wind at 20 hPa reveals a strong seasonal persistence from November to June/July. Ozone anomalies in layer 3 show a very similar seasonal persistence from November/December up to July. This similarity and the strong correlations between ozone anomalies in layer 3 and zonal wind at 20 hPa, together with our understanding of the synchronous QBO ozone signal associated with the QBO-induced meridional circulation, support our hypothesis that the persistence in ozone is caused by the persistence in zonal wind. Correspondingly, the ozone anomalies in layer 2 are highly correlated with the zonal wind at 40 hPa, and again, both fields show very similar seasonal persistence.

[25] As a final test of our hypothesis, we use a linear regression model to separate the QBO-related variability in ozone from the variability that cannot be explained by the QBO signal. Using the output from the linear regression model, we are able to derive the ozone anomalies associated with the QBO signal as a linear combination of the two orthogonal QBO time series based on observed stratospheric winds. The residual ozone time series is calculated as the difference between the original ozone and the QBO ozone time series. The variability of the residual ozone time series is related to other sources of variability such as the solar cycle and ENSO, as well as to unexplained ozone variability. In order to analyze if the residual time series is characterized by a seasonal persistence, we calculate the correlations between the monthly mean residual ozone time series. Figure 5 shows the correlation coefficients for the residual ozone time series of layer 3 and of layer 2. Clearly, the time series of the residuals are not characterized by a seasonal persistence of their anomalies. In layer 3, the anomalies only persist for a very short time (1–2 months), while in layer 2, the persistence is slightly longer (approximately 3 months). Moreover, the layers do not show preferred seasons for enhanced or reduced persistence of the anomalies. This supports our hypothesis that the seasonal persistence of the original time series of ozone anomalies is caused by the seasonal persistence of the QBO signal itself. As soon as the variability associated with the QBO signal is

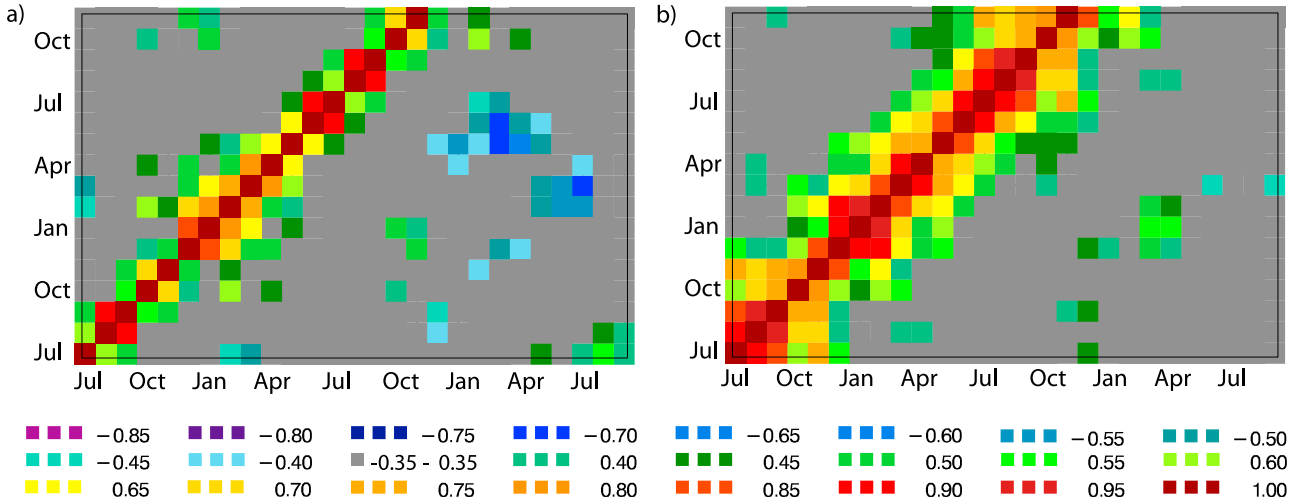

Figure 5. Correlation coefficients for ozone residuals averaged over 5°S–5°N for the SAGE-corrected SBUV data set between monthly mean time series in (a) layer 3 and (b) layer 2. Ozone variability associated with the QBO has been removed from the ozone residual time series using linear regression analysis.

removed from the ozone time series, the seasonal persistence vanishes.

3.2. Ozone Persistence in the Equatorial Upper Stratosphere

[26] We now analyze the persistence of equatorial ozone anomalies in the upper stratosphere, where ozone is under photochemical control. Figure 6a shows the correlation coefficients between the monthly mean ozone anomaly time series of layer 7 (6–4 hPa), which is part of the upper stratosphere. There is a time frame, starting in October and ending in May, during which the monthly mean ozone time series are highly correlated with each other.

[27] Overall, the correlations for layer 7 are very similar to the ones found for layer 3 (shown in Figure 2a), with the time frame of high correlation coefficients shifted by only 1 month. Correlations between ozone anomalies in layer 3 and layer 7 are shown in Figure 6b. In general, the ozone anomalies of the two layers are positively correlated. A given phase of the QBO leads to ozone anomalies of opposite sign in the lower and upper stratosphere. Since the QBO phase propagates downward with time these anomalies are lagged by approximately 1 year. At any one point in time, it is common to see positive (negative) anomalies in both the upper and lower stratosphere due to the fact that while the lower stratosphere is in one phase of the QBO the upper stratosphere is in the next phase. This leads to a

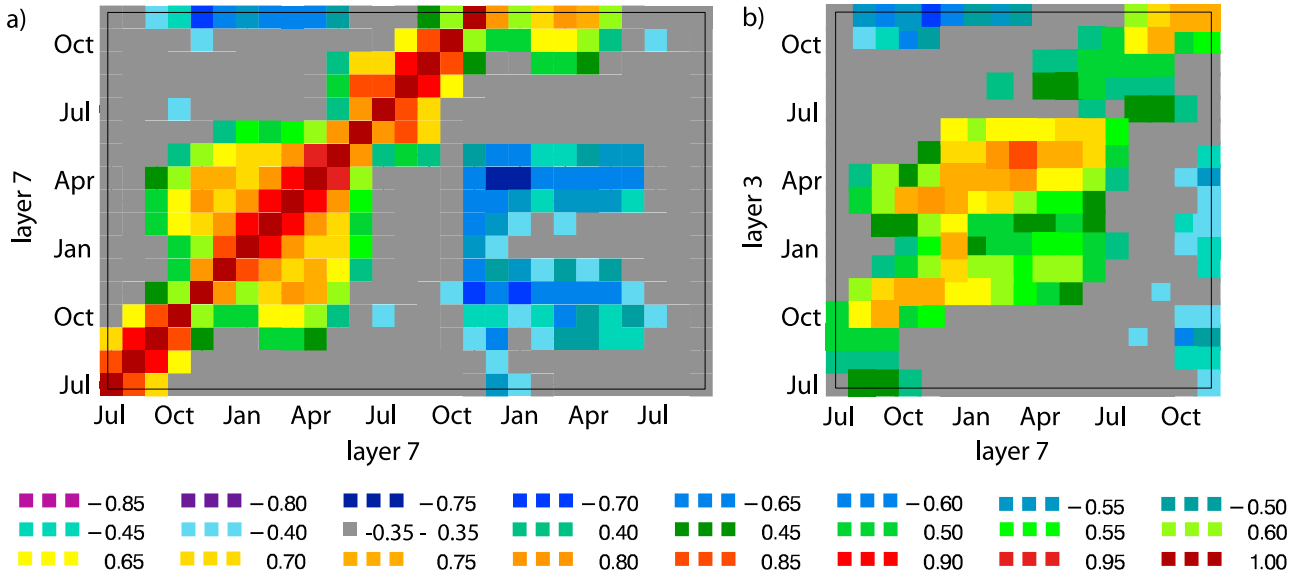

Figure 6. Correlation coefficients for ozone averaged over 5°S–5°N for the SAGE-corrected SBUV data set between monthly mean time series in (a) layer 7 and (b) layer 7 and layer 3. Each field represents the correlation between the ozone time series for two particular months, as labeled.

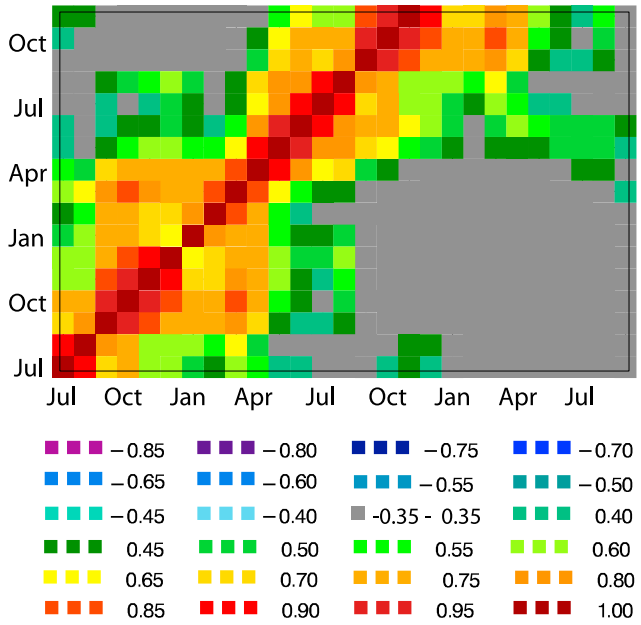

Figure 7. Correlation coefficients for ERA-40 temperature averaged over 5°S–5°N between monthly mean time series at 5 hPa. Each field represents the correlation between the temperature time series for two particular months, as labeled.

positive correlation between the partial ozone columns in layer 3 and layer 7 as seen in Figure 6b. Surprisingly, the correlation has a marked seasonal dependence, being especially strong in the time frame from November until June and rather weak during the months from July to October. The correlations between layer 3 and layer 7 in Figure 6b are strong during exactly the same time of year when both layers show the seasonal persistence of their anomalies.

[28] We hypothesize that analogous to the equatorial lower stratosphere, the upper stratospheric QBO signal is characterized by a seasonal persistence, which causes the seasonal persistence of ozone anomalies. Unfortunately, radiosonde measurements of equatorial winds are not available above 10 hPa. However, temperature data are available for the upper stratosphere and zonal-mean temperature is directly related to the vertical zonal-mean wind shear so that it can be used as a proxy for the zonal QBO winds. (We choose to use reanalysis temperature rather than reanalysis winds in the upper stratosphere because the reanalysis is based on temperature measurements in this region.) The interannual variability of zonal-mean equatorial temperature in this region is dominated by the QBO signal (not shown here). Figure 7 shows the correlation coefficients between the monthly mean equatorial temperature time series at 5 hPa. The temperature anomalies for all the months from September onward are highly correlated with the temperature anomalies in the following months up to April, after which the correlation coefficients drop off. This seasonal persistence of upper stratospheric temperature anomalies indicates that the QBO signal in zonal wind is also characterized by a seasonal persistence in the upper stratosphere. Furthermore, the time frame of the seasonal persistence is virtually the same as that for the ozone anomalies in layer 7. This supports the hypothesis that, as in the lower stratosphere, the seasonal persistence of the upper stratospheric ozone anomalies results from the seasonal persistence of the QBO itself.

[29] As an additional test of the hypothesized link between the seasonal persistence of the QBO and that of ozone, we repeated the analysis of Figure 5 for the residual time series of upper stratospheric ozone anomalies. The residual time series were derived by removing the variability associated with the QBO signal. The correlation coefficients for the residual ozone time series (not shown here) display no clear pattern of clustered high correlation coefficients. Therefore, as for the lower stratosphere, the residual time series in the upper stratosphere shows no preferred season for enhanced or reduced persistence. This indicates that the seasonal persistence of upper stratospheric ozone anomalies is caused by the seasonal persistence of the QBO signal.

[30] Although the seasonal persistence of ozone anomalies in layer 3 and layer 7 is in both cases linked to the seasonal persistence of the QBO signal, these links are based on different physical mechanisms. It is well known that while ozone anomalies in the lower stratosphere are caused by QBO-induced variability of ozone transport, ozone in the upper stratosphere is under photochemical control and the direct influence of transport on ozone is negligible. The effect of the QBO-induced temperature signal on the reaction rates controlling ozone destruction has been identified as one source of the ozone QBO signal in the photochemically controlled region [*Ling and London*, 1986; *Zawodny and McCormick*, 1991]. In addition to the temperature influence, the QBO-induced variability of NO_y transport that affects ozone chemically through NO_x is important in forcing the ozone QBO [*Chipperfield et al.*, 1994; *Tian et al.*, 2006]. Indeed, *Tian et al.* [2006] found from their coupled chemistry-climate model (CCM) simulations that around 35 km the variations in NO_x are the main contributor to the ozone QBO, with the temperature variations contributing only about 20% of the signal. However, the CCM study of *Butchart et al.* [2003] exhibited an ozone QBO in the upper stratosphere even when NO_y was held fixed, and *Randel and Wu* [1996] showed that the strong negative correlations between observed ozone and NO_x anomalies drop off rapidly with increasing altitude above 35 km. In general, both temperature and NO_x variations affect ozone in the photochemically controlled region. It is reasonable to assume that the NO_x variations contribute the dominant forcing between 30 and 35 km, with rapidly decreasing importance at higher altitudes as the relative role of the NO_x ozone-destruction cycles diminishes and the more temperature-sensitive O_x cycles play a larger role [*Brasseur and Solomon*, 2005]. The relevance of temperature variations for inducing ozone variations is manifested in the general anticorrelation observed between ozone and temperature in the upper stratosphere [e.g., *Ward et al.*, 2000].

[31] The seasonal persistence of the QBO can be seen in the seasonal persistence of the equatorial temperature anomalies (Figure 7), which, through the mechanism of the persistence of photochemical perturbations to ozone, can lead to the persistence of ozone anomalies. On the basis of the altitude-dependent balance between NO_x and temperature effects on ozone, we expect this mechanism to be an important contributor to the seasonal persistence of ozone anomalies above the region of NO_x control. We hypothesize

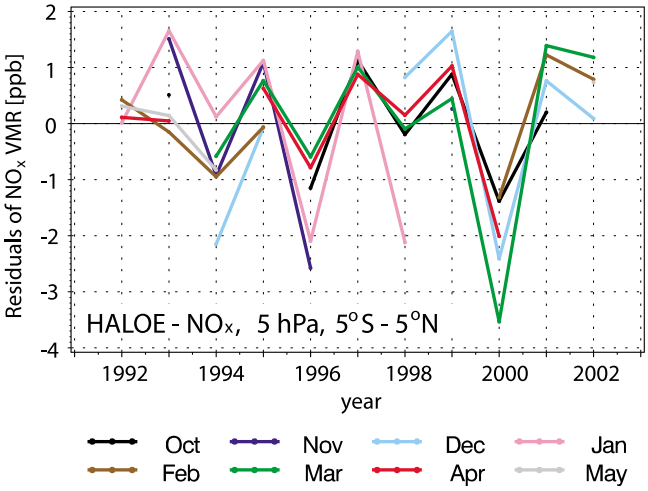

Figure 8. Time series of NO_x anomalies at 5 hPa averaged over 5°S–5°N equivalent latitude for HALOE. The 8 months from October until May of the following year are shown.

that in the region of NO_x control, the seasonal persistence of ozone anomalies is mainly caused by the seasonal persistence of QBO-induced NO_y (and thereby NO_x) anomalies. In order to test this hypothesis, we first have to investigate the persistence of NO_x anomalies in the equatorial upper stratosphere. Figure 8 shows the year-to-year variability of HALOE NO_x anomalies at 5 hPa averaged over 5°S–5°N equivalent latitude for the months from October to May of the following year. The individual months show some data gaps for a number of years. In general, the number of years is too small to calculate meaningful correlation coefficients between the time series, so we adopt a qualitative approach. The interannual NO_x anomalies do not change their magnitude during the months shown here and clearly persist from October through May, which is essentially the same time frame that exhibits persistence of 5 hPa QBO-induced temperature anomalies. The analysis of NO_x time series thus indicates that the seasonal persistence of transport-induced NO_y anomalies is caused by the seasonal persistence of the QBO itself.

[32] Ozone anomalies in layer 7 correspond to the partial ozone column between 6 and 4 hPa (around 35–37 km). We have provided evidence of the seasonal persistence of both equatorial temperature anomalies and NO_x anomalies at 5 hPa, which is somewhere within the region where ozone changes from NO_x control to temperature control. In order to investigate the relative importance of the seasonal persistence of temperature and NO_x anomalies for the seasonal persistence of ozone anomalies at 5 hPa, we calculate the correlation coefficients between equatorial anomalies of SAGE II ozone, SAGE II NO_2, HALOE NO_x, and ERA-40 temperature at 5 hPa. Since the relation between ozone, temperature, and NO_x changes rapidly with altitude, it is necessary to calculate the correlation coefficients between ozone and temperature given at exactly the same level. For this reason, we use SAGE II ozone given at the pressure level 5 hPa instead of the merged SAGE-corrected SBUV ozone given as the partial ozone column between 6 and 4 hPa. Note that the correlation between SAGE-corrected SBUV ozone in layer 7 and SAGE II ozone at 5 hPa is very high (0.8) and the two time series show a very similar variability. The correlation coefficients are calculated based on the time series over all the months and years and given in Table 1. Whereas ozone and temperature show a clear anticorrelation, ozone and NO_2 are not correlated and ozone and NO_x are only weakly anticorrelated. This indicates that at 5 hPa, temperature contributes the dominant forcing of the ozone anomalies. Note that temperature and NO_2 as well as temperature and NO_x are not correlated at 5 hPa. To illustrate the altitude dependence of the balance between temperature and NO_x effects on ozone, we look at the correlation coefficients between SAGE II ozone, SAGE II NO_2, HALOE NO_x, and ERA-40 temperature at 10 hPa, which are given in Table 2. Now the anticorrelations between ozone and NO_2 and between ozone and NO_x are high, whereas ozone is only weakly correlated with temperature. Comparison of the correlation coefficients at 10 and 5 hPa illustrates that while NO_x dominates at 10 hPa, temperature seems to be more important at 5 hPa. Therefore, the seasonal persistence of ozone anomalies in layer 7 is very likely caused by the seasonal persistence of temperature anomalies.

3.3. Ozone Persistence in the Transition Zone Between 16 and 10 hPa

[33] In general, ozone in layer 5 (16–10 hPa) is of particular interest since this region, which represents the transition between the dynamically and photochemically controlled regions, serves as the primary supply region of ozone to the extratropical lower stratosphere [*Brasseur and Solomon*, 2005]. The maximum in the vertical profile of equatorial ozone mixing ratio occurs between 15 and 5 hPa, with layer 5 being part of this region. Ozone anomalies in layer 5 show the smallest standard deviations compared to other layers, as is apparent from Figure 1. It is likely that the QBO ozone signal caused by the chemical effects of NO_y and the signal caused by ozone transport cancel each other out in the transition zone between the dynamically and photochemically controlled regions, leading to the observed weak variability. The correlation coefficients between the

Table 1. Correlation Coefficients Between Monthly Mean SAGE II Ozone, SAGE II NO_2, HALOE NO_x, and ERA-40 Temperature Anomalies Averaged Over 5°S–5°N at 5 hPa and *P* Value Under the Null Hypothesis of Zero Correlation[a]

	O_3	NO_2	NO_x	Temperature
O_3	1	−0.15 $P < 0.0675$	−0.32 $P < 0.0103$	−0.7 $P < 0.0001$
NO_2		1	0.38 $P < 0.0102$	0.01 $P < 0.9153$
NO_x			1	0.13 $P < 0.24878$
Temperature				1
Standard deviation	0.5 ppm	0.6 ppb	0.75 ppb	2.86 K

[a]The correlation coefficients are calculated based on the time series over all the months and years, and the standard deviation for each time series is given in the last row of the table.

Table 2. Correlation Coefficients Between Monthly Mean SAGE II Ozone, SAGE II NO_2, HALOE NO_x, and ERA-40 Temperature Anomalies Averaged Over 5°S–5°N at 10 hPa and *P* Value Under the Null Hypothesis of Zero Correlation[a]

	O_3	NO_2	NO_x	Temperature
O_3	1	−0.76 $P < 0.0001$	−0.64 $P < 0.0001$	−0.42 $P < 0.0001$
NO_2		1	0.63 $P < 0.0001$	0.29 $P < 0.0003$
NO_x			1	0.44 $P < 0.0001$
Temperature				1
Standard deviation	0.51 ppm	0.83 ppb	1.16 ppb	1.15 K

[a]The correlation coefficients are calculated based on the time series over all the months and years, and the standard deviation for each time series is given in the last row of the table.

equatorial monthly mean ozone time series for layer 5 are shown in Figure 9a. A very strong seasonal persistence is apparent for the time frame from June/July to December. After December, the coefficients drop from high values around 0.7 to values that are not statistically significant. Note that this time frame of seasonal persistence is almost opposite to that found for the lower and upper stratosphere. Moreover, there is no anticorrelation between the ozone anomalies separated by 1 year as was seen for layers 3 and 7, where the QBO signal is strong. The correlations with layer 7 (not shown here) are relatively weak with correlation coefficients between 0.4 and 0.6 found for a time shift of half a year. All the above characteristics observed for the correlations of layer 5 indicate that ozone anomalies in the narrow transition zone between chemical and dynamical control (16–10 hPa) show completely different characteristics than ozone anomalies in the lower (40–25 hPa) or upper (6–4 hPa) stratosphere. Therefore, it is not surprising that the ozone anomalies of layer 5 do not show persistence from autumn to the following spring as do the ozone anomalies in layers 3 and 7.

[34] Since ozone in layer 5 is less influenced by the QBO than in the other stratospheric layers, we would not expect that the seasonal persistence of the QBO signal causes the seasonal persistence of the ozone anomalies in layer 5. In order to investigate the question of whether the seasonal persistence of ozone anomalies in layer 5 is influenced by the seasonal persistence of zonal winds, we analyze the residual time series with QBO variability removed. Figure 9b shows the correlation coefficients for the residual ozone time series of layer 5. The correlation has a marked seasonal dependence being especially strong from July to November and rather weak during the rest of the year. Overall, the correlations for the residual ozone time series and those for the original ozone anomalies are very similar, except for December, which shows no seasonal persistence for the residual time series. This similarity is in contrast to the results found for the lower and upper stratosphere, where the residual anomalies showed no seasonal persistence, and therefore the seasonal persistence could be associated with the QBO signal in ozone. In the transition zone between the lower and upper stratosphere, however, the ozone persistence shows a very different seasonal structure and is not associated with the QBO signal in ozone.

4. Summary

[35] Analysis of ozone profile data has demonstrated that the seasonal persistence of ozone anomalies is not only a phenomenon of the extratropics, where ozone variability is modulated by the QBO and synchronized with the seasonal cycle [*Tegtmeier et al.*, 2008], but is also a characteristic of the equatorial region where ozone variability is dominated by the QBO signal.

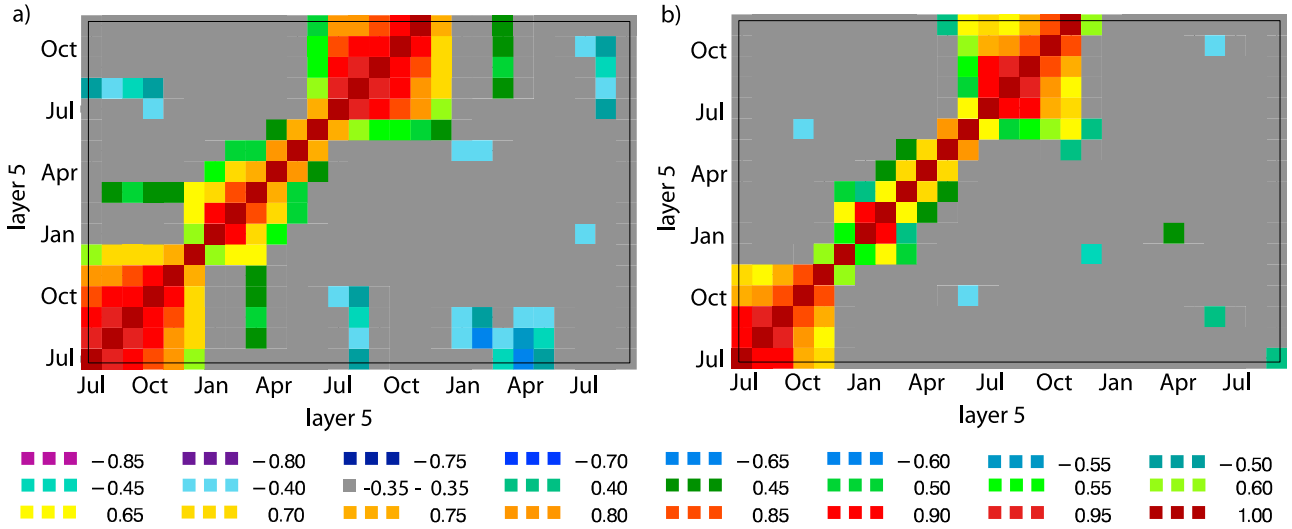

Figure 9. Correlation coefficients for ozone averaged over 5°S–5°N for the SAGE-corrected SBUV data set between monthly mean time series in (a) layer 5 and (b) layer 5 ozone residuals with the QBO-related variability removed as in Figure 5. Each field represents the correlation between the ozone time series for two particular months, as labeled.

[36] Maximum equatorial ozone variability occurs in the lower stratosphere (40–25 hPa) and in the upper stratosphere (6–4 hPa). This study has shown that ozone anomalies within these two stratospheric regions persist from approximately November until June of the following year. During the time frame of their seasonal persistence, ozone anomalies in each layer are highly correlated from month to month and show strong anticorrelations with ozone anomalies lagged by approximately 1 year. For both regions, analysis of the ozone time series with QBO variability removed confirms that the seasonal persistence of ozone anomalies is associated with the QBO signal in ozone.

[37] Our study suggests that the ozone anomaly persistence in the lower and upper stratosphere depends on the seasonal persistence of the QBO-induced meridional circulation and therefore on the seasonal persistence of the QBO itself. This hypothesis was supported by analysis of zonal winds in the lower stratosphere, which display a strong seasonal persistence. Additionally, high correlations between zonal wind and ozone anomalies for the respective layers with the same pattern of seasonal persistence point to the mechanism of persistence of zonal winds causing the persistence of the ozone anomalies.

[38] Previous studies have recognized the tendency of the QBO phase transition to be synchronized to the annual cycle. Our analysis adds to this picture by demonstrating that not only the timing of the QBO phase transition but also the persistence of the QBO signal itself show a clear seasonal dependence. It is not known what mechanism causes the seasonality of QBO phase transitions. One possible mechanism is based on the seasonal modulation of the rate of phase progression of the QBO, which is associated with the seasonal cycle in tropical upwelling. However, the time frame of seasonal persistence of the zonal wind anomalies is different for different layers, suggesting that there is no simple relationship with the seasonal cycle in tropical upwelling.

[39] The seasonal persistence of ozone anomalies in the upper stratosphere cannot be explained by the effects of the QBO-induced meridional circulation on the transport of ozone, since the lifetime of O_x is too short in this region. Rather, ozone anomalies are induced chemically by a combination of temperature anomalies and transport-related NO_y anomalies. It is suggested that, analogous to the lower stratosphere, the upper stratospheric QBO is characterized by a seasonal persistence that causes the seasonal persistence of anomalies in temperature and in long lived trace gases such as NO_y. Evidence for this mechanism has been provided by the analysis of both temperature and NO_x time series. Our study suggests that while around 5 hPa the ozone anomalies are caused mainly by temperature anomalies, at 10 hPa, the ozone anomalies are caused mainly by NO_x anomalies.

[40] *Tegtmeier et al.* [2008] analyzed NH extratropical ozone anomalies and found that the partial ozone column above 16 hPa shows especially strong seasonal persistence. The study argued that this persistence arose from the persistence of transport-induced wintertime anomalies in NO_y, which perturb ozone through NO_x chemistry. Note that the mechanisms for the persistence of ozone anomalies at the equator and in the extratropics are quite different. The QBO signal in extratropical ozone is especially strong in winter and early spring since the QBO affects the dynamical forcing of the Brewer-Dobson circulation during this time of the year. During the summertime period, transport becomes much less important and hence so does the synchronous influence of the QBO on extratropical ozone anomalies, as is reflected by the small correlations between equatorial wind and extratropical ozone in summer and autumn. Through the "seasonal memory" of extratropical NO_y anomalies, the QBO has an asynchronous effect on subtropical ozone in the upper stratosphere during summer and early autumn. In the equatorial region, on the other hand, ozone anomalies are highly correlated with the equatorial winds through the whole year. In this region, the seasonal persistence of ozone anomalies is caused by the seasonal persistence of the QBO itself.

[41] Between the two stratospheric layers of maximum equatorial ozone variability, ozone anomalies are small and less dominated by the QBO signal. The latter characteristic is illustrated by the lack of anticorrelations between ozone anomalies separated by 1 year. Nevertheless, this layer is important as it represents the transition between the dynamically and photochemically controlled regions and serves as the primary supply region of ozone to the extratropical lower stratosphere [*Brasseur and Solomon*, 2005]. Analysis of equatorial ozone anomalies in this stratospheric region (16–10 hPa) demonstrates a strong seasonal persistence from June to December. Analysis of the ozone time series with the QBO variability removed shows that the seasonal persistence is not associated with the QBO signal. Overall, ozone anomalies in the narrow transition zone between chemical and dynamical control (16–10 hPa) behave very differently compared to ozone anomalies in the broad regions above and below.

[42] **Acknowledgments.** The authors would like to thank NASA Goddard, NASA Langley Research Center (NASA-LaRC), and NOAA for making SAGE, SBUV, and HALOE data available. S.T. especially acknowledges the Canadian Natural Sciences and Engineering Research Council postdoctoral fellowship allowing this study to be completed. T.G.S. is supported by the Natural Sciences and Engineering Research Council, the Canadian Foundation for Climate and Atmospheric Sciences, and the Canadian Space Agency.

References

Anstey, J. A., and T. G. Shepherd (2008), Response of the northern stratospheric polar vortex to the seasonal alignment of QBO phase transitions, *Geophys. Res. Lett.*, *35*, L22810, doi:10.1029/2008GL035721.

Baldwin, M. P., et al. (2001), The quasi-biennial oscillation, *Rev. Geophys.*, *39*, 179–229.

Bhartia, P. K., C. G. Wellemeyer, S. L. Taylor, N. Nath, and A. Gopolan (2004), Solar backscatter ultraviolet (SBUV) version 8 profile algorithm, paper presented at Quadrennial Ozone Symposium, Int. Ozone Comm., Kos, Greece.

Bowman, K. P. (1989), Global patterns of the quasi-biennial oscillation in total ozone, *J. Atmos. Sci.*, *46*, 3328–3343.

Brasseur, G., and S. Solomon (2005), *Aeronomy of the Middle Atmosphere*, 2nd ed., Springer, New York.

Butchart, N., A. A. Scaife, J. Austin, S. H. E. Hare, and J. R. Knight (2003), Quasi-biennial oscillation in ozone in a coupled chemistry-climate model, *J. Geophys. Res.*, *108*(D15), 4486, doi:10.1029/2002JD003004.

Campbell, L. J., and T. G. Shepherd (2005), Constraints on wave drag parameterization schemes for simulating the quasi-biennial oscillation. Part I: Gravity wave forcing, *J. Atmos. Sci.*, *62*, 4178–4195.

Chipperfield, M. P., L. J. Gray, J. S. Kinnersley, and J. Zawodny (1994), A two-dimensional model study of the QBO signal in SAGE II NO_2 and O_3, *Geophys. Res. Lett.*, *21*, 589–592.

Cunnold, D. M., W. P. Chu, R. A. Barnes, M. P. McCormick, R. E. Veiga, D. Murcray, N. Iwagami, K. Shibasaki, P. C. Simon, and W. Peetermans (1989), Validation of SAGE II ozone measurements, *J. Geophys. Res.*, *94*, 8447–8460.

Dunkerton, T. J. (1990), Annual variation of deseasonalized mean flow acceleration in the equatorial lower stratosphere, *J. Meteorol. Soc. Jpn*, *68*, 499–508.

Dunkerton, T. J., and D. P. Delisi (1985), Climatology of the equatorial lower stratosphere, *J. Atmos. Sci.*, *42*, 376–396

Fioletov, V. E., and T. G. Shepherd (2003), Seasonal persistence of midlatitude total ozone anomalies, *Geophys. Res. Lett.*, *30*(7), 1417, doi:10.1029/2002GL016739.

Fioletov, V. E., D. W. Tarasick, and I. Petropavlovskikh (2006), Estimating ozone variability and instrument uncertainties from SBUV(/2), ozonesonde, Umkehr, and SAGE II measurements: Short-term variations, *J. Geophys. Res.*, *111*, D02305, doi:10.1029/2005JD006340.

Frith, S., R. Stolarski, and P. K. Bhartia (2004), Implications of version 8 TOMS and SBUV data for long-term trend analysis, paper presented at Quadrennial Ozone Symposium, Int. Ozone Comm., Kos, Greece.

Funk, J. P., and G. L. Garnham (1962), Australian ozone observations and a suggested 24 month cycle, *Tellus*, *14*, 378–382.

Fusco, A. C., and M. L. Salby (1999), Interannual variations of total ozone and their relationship to variations of planetary wave activity, *J. Clim.*, *12*, 1619–1629.

Grooß, J.-U., and J. M. Russell III (2005), Technical note: A stratospheric climatology for O_3, H_2O, CH_4, NO_x, HCl and HF derived from HALOE measurements, *Atmos. Chem. Phys.*, *5*, 2797–2807.

Hasebe, F. (1983), Interannual variations of global total ozone revealed from Nimbus 4 BUV and ground-based observations, *J. Geophys. Res.*, *88*, 6819–6834.

Hasebe, F. (1994), Quasi-biennial oscillation of ozone and diabatic circulation in the equatorial stratosphere, *J. Atmos. Sci.*, *51*, 729–745.

Holton, J. R., and H.-C. Tan (1980), The influence of the equatorial quasi-biennial oscillation on the global circulation at 50 mb, *J. Atmos. Sci.*, *37*, 2200–2208.

Ling, X. D., and J. London (1986), The quasi-biennial oscillation of ozone in the tropical middle stratosphere: A one-dimensional model, *J. Atmos. Sci.*, *43*, 3122–3137.

McCormick, M. P., J. M. Zawodny, R. E. Veiga, J. C. Larsen, and P.-H. Wang (1989), An overview of SAGE I and II ozone measurements, *Planet. Space Sci.*, *37*, 1567–1586.

McLinden, C. A., S. Tegtmeier, and V. E. Fioletov (2009), Technical Note: A combined SBUV and SAGE zonal mean data set, *Atmos. Chem. Phys.*, *9*, 7963–7972.

Naujokat, B. (1986), An update of the observed quasi-biennial oscillation of the stratospheric winds over the tropics, *J. Atmos. Sci.*, *43*, 1873–1877.

Pascoe, C. L., L. J. Gray, S. A. Crooks, M. N. Juckes, and M. P. Baldwin (2005), The quasi-biennial oscillation: Analysis using ERA-40 data, *J. Geophys. Res.*, *110*, D08105, doi:10.1029/2004JD004941.

Ramanathan, K. R. (1963), Bi-annual variation of atmospheric ozone over the tropics, *Q. J. R. Meteorol. Soc.*, *89*, 540–542.

Randel, W. J., and J. B. Cobb (1994), Coherent variations of monthly mean column ozone and lower stratospheric temperature, *J. Geophys. Res.*, *99*, 5433–5447.

Randel, W. J., and F. Wu (1996), Isolation of the ozone QBO in SAGE II data by singular value decomposition, *J. Atmos. Sci.*, *53*, 2546–2559.

Randel, W. J., F. Wu, and R. Stolarski (2002), Changes in column ozone correlated with the stratospheric EP flux, *J. Meteorol. Soc. Jpn*, *80*, 849–862.

Rind, D., J. Lerner, and J. Zawodny (2005), A complementary analysis for SAGE II data profiles, *Geophys. Res. Lett.*, *32*, L07812, doi:10.1029/2005GL022550.

Russell, J. M., III, L. L. Gordley, J. H. Park, S. R. Drayson, D. H. Hesketh, R. J. Cicerone, A. F. Tuck, J. E. Frederick, J. E. Harries, and P. J. Crutzen (1993), The Halogen Occultation Experiment, *J. Geophys. Res.*, *98*, 10,777–10,797.

Tegtmeier, S., V. E. Fioletov, and T. G. Shepherd (2008), Seasonal persistence of northern low and middle latitude anomalies of ozone and other trace gases in the upper stratosphere, *J. Geophys. Res.*, *113*, D21308, doi:10.1029/2008JD009860.

Tian, W., M. P. Chipperfield, L. J. Gray, and J. M. Zawodny (2006), Quasi-biennial oscillation and tracer distributions in a coupled chemistry-climate model, *J. Geophys. Res.*, *111*, D20301, doi:10.1029/2005JD006871.

Tung, K. K., and H. Yang (1994), Global QBO in circulation and ozone. Part I: Reexamination of observational evidence, *J. Atmos. Sci.*, *51*, 2699–2707.

Uppala, S. M., et al. (2005), The ERA-40 reanalysis, *Q. J. R. Meteorol. Soc.*, *131*, 2961–3012.

Wallace, J. M., L. Panetta, and J. Estberg (1993), A phase-space representation of the equatorial stratospheric quasi-biennial oscillation, *J. Atmos. Sci.*, *50*, 1751–1762.

Wang, P.-H., D. M. Cunnold, C. R. Trepte, H. J. Wang, P. Jing, J. Fishman, V. G. Brackett, J. M. Zawodny, and G. E. Bodeker (2006), Ozone variability in the midlatitude upper troposphere and lower stratosphere diagnosed from a monthly SAGE II climatology relative to the tropopause, *J. Geophys. Res.*, *111*, D21304, doi:10.1029/2005JD006108.

Ward, W. E., J. Oberheide, M. Riese, P. Preusse, and D. Offermann (2000), Planetary wave two signatures in CRISTA 2 ozone and temperature data, in *Atmospheric Science Across the Stratopause*, *Geophys. Monogr. Ser.*, vol. 123, edited by D. E. Siskind, M. E. Summers, and S. D. Eckermann, pp. 319–325, AGU, Washington, D. C.

Weber, M., S. Dhomse, F. Wittrock, A. Richter, B. Sinnhuber, and J. P. Burrows (2003), Dynamical control of NH and SH winter/spring total ozone from GOME observations in 1995–2002, *Geophys. Res. Lett.*, *30*(11), 1583, doi:10.1029/2002GL016799.

World Meteorological Organization (2007), WMO scientific assessment of ozone depletion: 2006, *Rep. 50*, Global Ozone Res. and Monit. Proj., Geneva.

Zawodny, J. M., and M. P. McCormick (1991), Stratospheric Aerosol and Gas Experiment II measurements of the quasi-biennial oscillations in ozone and nitrogen dioxide, *J. Geophys. Res.*, *96*, 9371–9377.

V. E. Fioletov, Environment Canada, 4905 Dufferin St., Toronto, ON M3H 5T4, Canada.

T. G. Shepherd, Department of Physics, University of Toronto, 60 St. George St., Toronto, ON M5S 1A7, Canada.

S. Tegtmeier, Marine Meteorology, IFM-GEOMAR, Düsternbrooker Weg 20, D-24105 Kiel, Germany. (stegtmeier@ifm-geomar.de)